29th Congress of the International Council of the Aeronautical Sciences
St. Petersburg, Russia; September 7-12, 2014

EFFECT OF ELASTICITY IN THE BIRD-LIKE PRIMARY FEATHER WING ON THE FLIGHT STABILITY

Masahiro Motomatsu*, Yoshinobu Inada**
***Graduate School of Tokai University, ****Tokai University**

Keywords: Bird Wing, Primary Feather, Elasticity, Flight stability

Abstract

Birds in nature are capable of flying stably even in a turbulent flow. The micro air vehicle (MAV), however, has a serious problem of susceptibility to air turbulence although its size and weight are similar to those of birds. The primary feather in a bird wing can be a reason for the advanced stability. In this research, focusing on the elasticity in the primary feather of natural birds, the wind tunnel test was conducted for the rigid and elastic primary feather wing models and the aerodynamic performance of them were compared. In consequence, it was clarified that no conspicuous difference of C_L and C_D characteristics was found between those models, but the elastic primary feather model had a larger slope of side force and rolling moment coefficients with respect to the side slip angle than the rigid primary feather model, thus indicating the large flight stability of elastic primary feather wing in the lateral direction.

1 Introduction

The advantage of aerial information gathering by using micro air vehicles (MAV) is increasingly gaining a lot of attention recently. MAV has several merits e.g. low weight, low cost, low risk by crash, etc. However, MAV has a serious problem of susceptibility to air turbulence and thus flight stability is not sufficient. On the other hand, in nature, birds can fly in unstable air current and thus has high flight stability although its size and weight are small like MAV. It is considered that the primary feather of the wings of birds and its morphing characteristic, i.e. changeable form of wings according to a flight situation, are key factors. In the past, some researches on winglet which imitated the primary feather were conducted and the marked aerodynamic performance was pointed out, e.g. the reduction of induced drag and the improvement in a lift curve slope[1, 2]. However, the rigid wing made of wood or aluminum plates was used in these researches, and thus the effect of the elasticity of the feather which exists in a bird feather was not considered. On the other hand, Kawasaki et.al compared the wing with and without flexibility in the feathering rotation of the primary feather which was at the wing tip, and had pointed out that the primary feather with flexible feathering rotation had the high dihedral angle effect[3]. However, there was no elasticity in the primary feather itself. Therefore, in this research, the aerodynamic performance of primary feather with elasticity was investigated especially focusing on the flight stability and the comparison between the rigid and the elastic primary feather wing was conducted.

2 Method

In this research, the rigid primary feather wing was developed using four pieces of the aluminum plates of thickness 1.0[mm] as shown in Fig.1, and the elastic primary feather wings were developed using four pieces of plastic plates made of vinyl chloride of thickness 0.5[mm] and 0.8[mm] as shown in Figs. 2 and 3, respectively.

The aluminum plate has 11.7×10^{-2}[Nm^2] bending stiffness. The plastic plate of thickness 0.5[mm] and 0.8[mm] have 0.174×10^{-2}[Nm^2] and 0.622×10^{-2}[Nm^2] bending stiffness, respectively. The stainless plate of thickness 1.0

[mm] was stuck on the root of each plastic plate to be used for the fixing end. Four pieces of aluminum or plastic plate were fixed on the base made with two pieces of aluminum plate of thickness 0.5[mm] which sandwiched the fixing end of four plates. Four plates had same size at the beginning, but the intense flutter with bending and torsional vibration occurred in the plastic plates in the wind tunnel experiment. One of the reasons was the coincidence of natural frequency of four plates. Therefore the size of four plates was altered in the final experimental model, i.e. 30[mm]×110[mm], 30[mm]×120[mm], 30[mm] ×130[mm], and 30[mm]×140[mm]. The angle of the gap between the plates was altered to analyze the aerodynamic effect of gap, i.e. 5[deg], 10[deg], and 15[deg]. Symmetrical primary feather wings were developed and were set at both tips of the wing which was the conventional type of air plane wing as shown in Fig. 4.

In the wind tunnel experiment, lift, drag, side force, pitching moment, and rolling moment were measured. The angle of attack α was changed from -10[deg] to 28[deg] at 2[deg] intervals while the sideslip angle β was kept 0[deg] when the lift, the drag, and the pitching moment were measured. The sideslip angle β was changed from -30[deg] to 30[deg] at 5[deg] intervals while α was kept 5[deg] when the side force and the rolling moment were measured. Moreover, the wind velocity U was set 10[m/s] and 15[m/s]. Reynolds number for each wind velocity was 6.48×10^4 and 9.73×10^4, respectively.

3 Results and Discussion

Among the measured aerodynamic force, the change of the lift coefficient C_L and the drag coefficient C_D to the angle of attack α for various gap angles is shown in Figs. 5-7 and Figs. 8-10, respectively. In Figs. 5-7, C_L continues increasing to near the angle of attack 10[deg], and decreases a little after that, taking an almost constant value. Therefore, it is confirmed that the stalling behavior is good. Moreover, it turns out that there is no large difference between the aluminum and the elastic primary feather wings. In Figs. 8-10, there is also no large difference between the aluminum and the elastic primary feather wings in C_D. Next, the graph of lift-drag ratio C_L/C_D which is a ratio of lift to drag is shown in Figs. 11-13. Although C_L/C_D takes the maximum near the angle of attack 5[deg] and the magnitude changes among the gap angles, it turns out that there is no large difference between the aluminum and the elastic primary feather wings.

The side force coefficient C_y and the rolling moment coefficient C_l to the sideslip angle β are shown in Figs. 14-16 and Figs. 17-19, respectively. When sideslip angle β has a large negative or positive value, there is a tendency for the elastic primary feather wing to have the larger absolute value of C_y and C_l than that of the aluminum primary feather wing, and this tendency is largest in the softest primary feather wing with thickness 0.5[mm]. In order to make this tendency clearer, the absolute value of the slope, i.e. $|C_{y\beta}|$ and $|C_{l\beta}|$, near the origin of each graph was calculated, and is shown in Figs. 20 and 21, respectively. It is confirmed from these figures that elastic primary feather wing tend to have a larger slope and the wing with large angle of gap between plates also tends to have a larger slope. The value of $|C_{y\beta}|$ means the

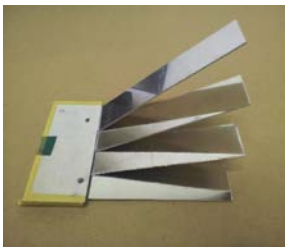

Fig. 1 Rrigid primary feather wing (aluminum)

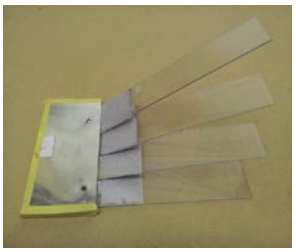

Fig. 2 Plastic primary feather wing (thickness 0.5[mm])

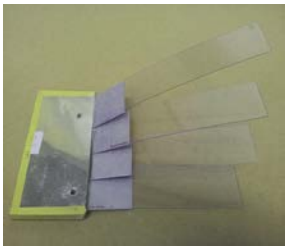

Fig. 3 Plastic primary feather wing (thickness 0.8[mm])

Fig. 4 Model with primary feather wings

magnitude of the braking force to the sideslip as shown in Fig. 22. Therefore, the elastic primary feather wing with large gap between plates which has the large $|C_{y\beta}|$ can make effective braking force to the sideslip and thus can realize the marked straight line flight stability. Moreover, the value of $|C_{l\beta}|$ means the magnitude of the restoration moment by the dihedral angle effect which occurs to the sideslip as shown in Fig. 22. Therefore, the elastic primary feather wing with large gap between plates which has the large $|C_{l\beta}|$ can also make large restoration moment to the sideslip and thus can inhibit the divergence of role, contributing to the straight line flight stability.

The reasons of above results are considered as follows: in the plastic plate, it bends up by elastic deformation as shown in Fig. 23, and this bending may become conspicuous when it receives the lateral wind during sideslip. This causes the increase of side area, and thus the side force coefficient C_y and its slope $|C_{y\beta}|$ may be increased. This bending up also increases the dihedral angle of the plastic plate, resulting in the increase of C_l and $|C_{l\beta}|$ as a consequence of the augmented dihedral angle effect. However, Dutch roll may be easy to generate because of the increased restoration moment when the dihedral angle is too large, and the influence of a gust blowing laterally may be conspicuous because of the increased side area, thus disturbing the stability of flight in the turbulent wind. It is thought that the bird may handle these problems by controlling the angle of the tail and the wing itself and/or inhibiting the bending of primary feather by contacting the muscle attaching to them. Although the similar countermeasures may be required when we apply the elastic primary feather wing to MAV, the augmented stability in the straight line flight will make it possible to arrive at a target point efficiently and take clear pictures with little blur under a small wind condition.

In order to confirm whether the high straight line flight stability is realized under the actual flight, we are now planning to conduct a flight test with a model glider equipped with elastic primary feather wings as shown in Fig. 24. The glider is made of expanded polystyrene; the primary feather wings are attached to the both wing tips; the length of the body of a glider is 830[mm]; the wingspan with the primary feather wings is 1500[mm]; the mean chord length of the wing is 120[mm]; thus the aspect ratio is 12.5. The microcomputer arduino (Arduino Pro Mini) and the 9 degrees of freedom sensor stick (SparkFun SEN-10724) with an accelerometer, a gyroscope sensor, and a direction sensor are combined together as shown in Fig. 25 (weight 87[g]) and mounted on the glider to be used as a data logger. This glider is launched by using a catapult with the same initial speed and the elevation angle for various cases as shown in Fig. 26. The experiments are now in progress.

4 Summary

In this study, the aerodynamic performance of rigid and elastic primary feather wing was compared by conducting the wind tunnel tests. The rigid and the elastic feather model were made of the aluminum plates and the plastic plates with various thickness to change the bending stiffness. The length of primary feathers was altered to prevent the flutter generation. The results of wind tunnel test clarified that the lift and the drag characteristics had no conspicuous difference between the rigid and the elastic primary feather wings, but elastic primary feather model had a larger slope of side force and rolling moment coefficients with respect to the side slip angle than the rigid primary feather model, thus indicating the high flight stability of elastic primary feather in the lateral direction.

References

[1] Cosin, R., Catalano, F.M., Correa, L.G.N., Entz, R.M.U., Aerodynamic Analysis of Multi-Winglets for Low Speed Aircraft, Proceedings of 27th International Congress of the Aeronautical Sciences (ICAS 2010) (2010)

[2] Smith, M. J., Komerath, N., Ames, R., Wong, O., Pearson, J., Performance Analysis of a Wing with Multiple Winglets, AIAA-paper AIAA-2001-2407 (2001).

[3] Y. Kawasaki, S. Ushiyama, M. Okamoto, Flight tests of Model Airplane Bird like Multiple Winglets, Proceedings of 29th Society of Aero Aqua Bio-mechanisms, p27-28 (2013).

Copyright Statement

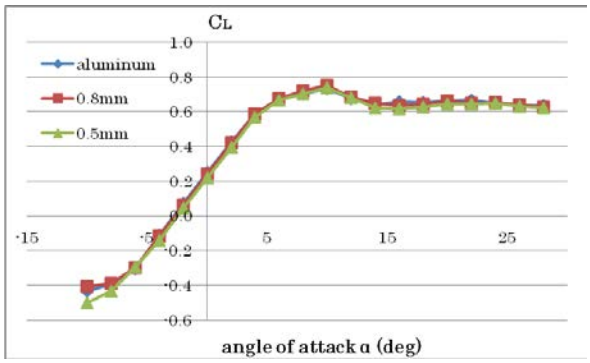

Fig. 5 C_L-α gap=5[deg], U=10[m/s]

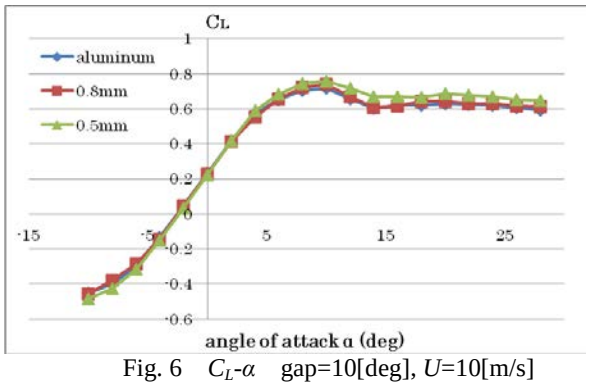

Fig. 6 C_L-α gap=10[deg], U=10[m/s]

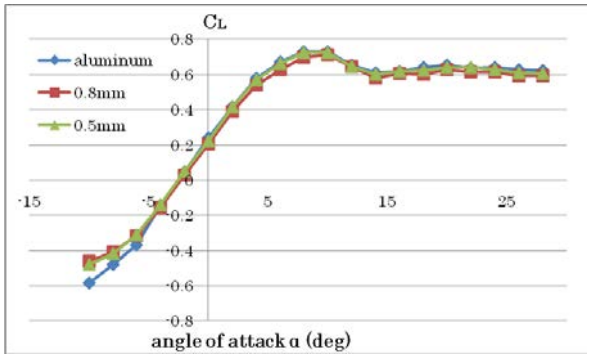

Fig. 7 C_L-α gap=15[deg], U=10[m/s]

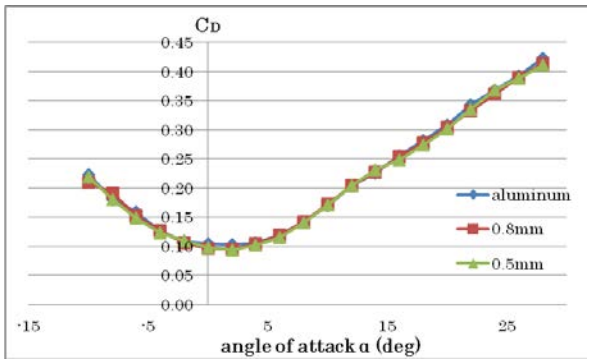

Fig. 8 C_D-α gap=5[deg], U=10[m/s]

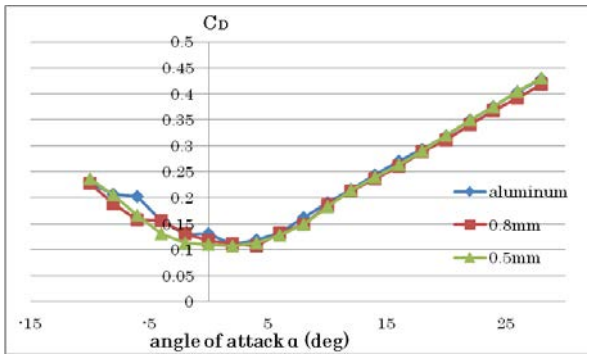

Fig. 9 C_D-α gap=10[deg], U=10[m/s]

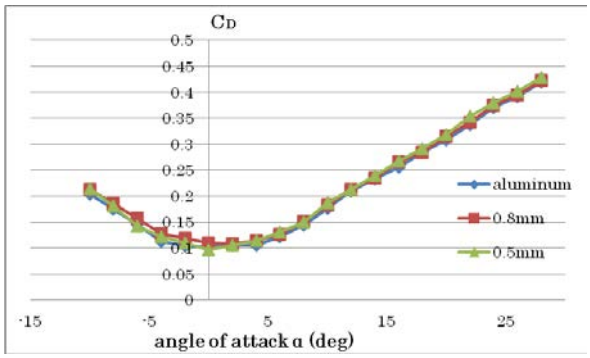

Fig. 10 C_D-α gap=15[deg], U=10[m/s]

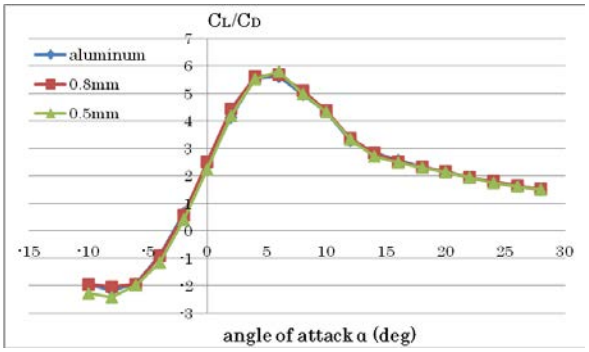

Fig. 11 C_L/C_D-α gap=5[deg], U=10[m/s]

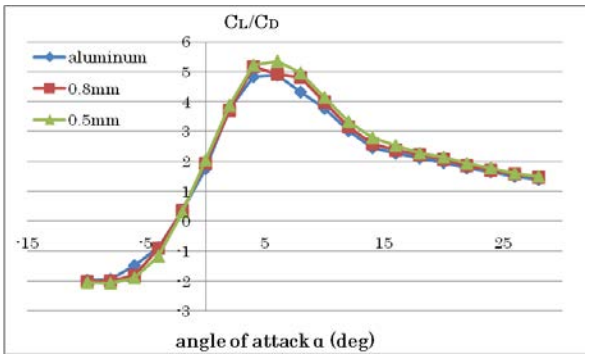

Fig. 12 C_L/C_D-α gap=10[deg], U=10[m/s]

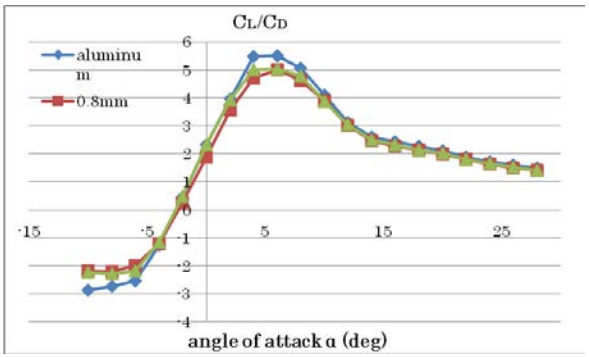

Fig. 13 C_L/C_D-α gap=15[deg], U=10[m/s]

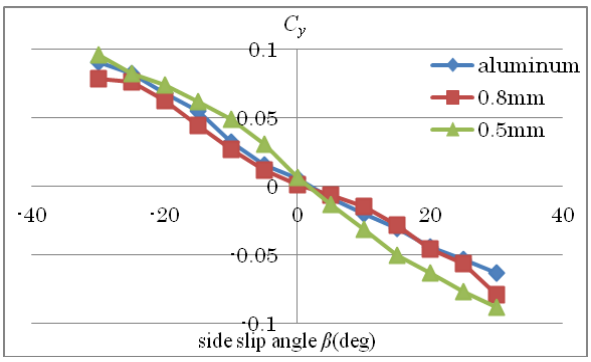

Fig. 14 C_y-β gap=5[deg], U=10[m/s]

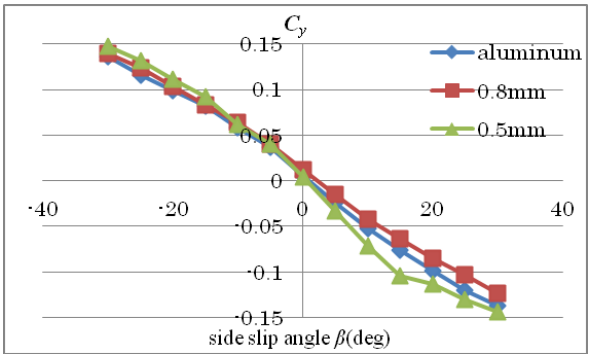

Fig. 15 C_y-β gap=10[deg], U=10[m/s]

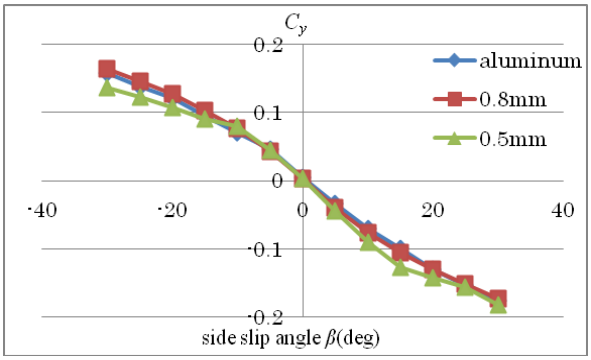

Fig. 16 C_y-β gap=15[deg], U=10[m/s]

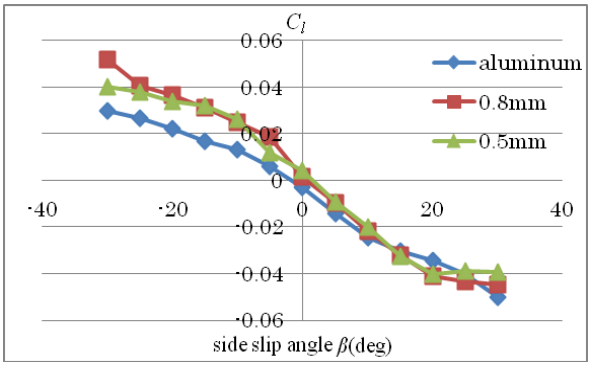

Fig. 17 C_l-β gap=5[deg], U=10[m/s]

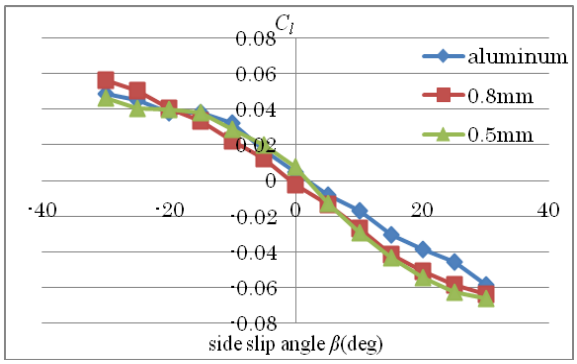

Fig. 18 C_l-β gap=10[deg], U=10[m/s]

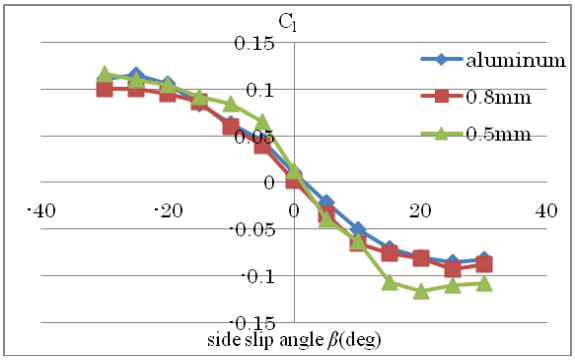

Fig. 19 C_l-β gap=15[deg], U=10[m/s]

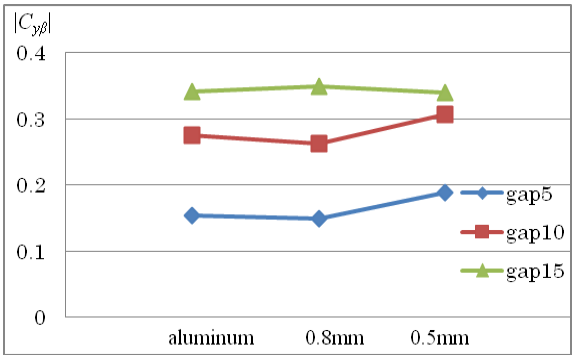

Fig. 20 Side force coefficient slope $|C_{y\beta}|$, U=10[m/s]

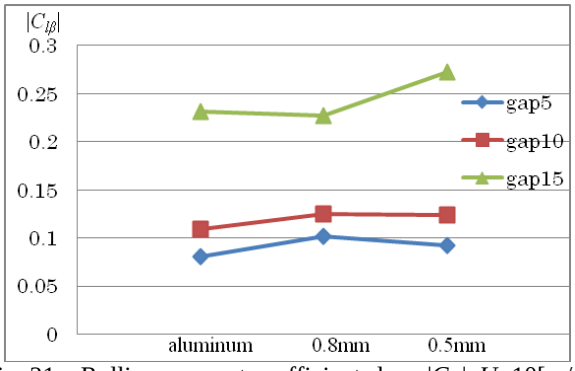

Fig. 21 Rolling moment coefficient slope $|C_{l\beta}|$, U=10[m/s]

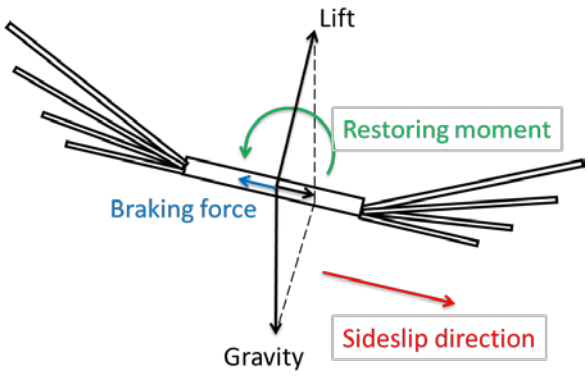

Fig. 22 The Braking force and the restoration moment generated in the sideslip

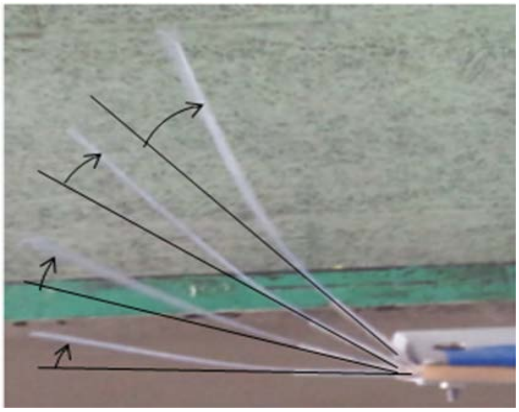

Fig. 23 Elastic deformation in primary feathers

Fig. 24 Glider with primary feather wings

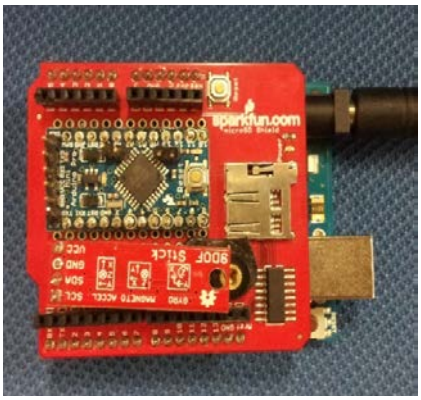

Fig. 25 Data logger

Fig. 26 Catapalt launch system